UDC 541.64 + 678.744

A.N.Klivenko[1], G.S.Tatykhanova[2, 3], Nurxat Nuraje[4], S.E.Kudaibergenov[2, 3]

[1]Al-Farabi Kazakh National University, Almaty;
[2]K.I.Satpayev Kazakh National Research Technical University, Almaty;
[3]Institute of Polymer Materials and Technology, Almaty;
[4]Department of Chemical Engineering, Texas Tech University, Lubbok, USA
(E-mail: skudai@mail.ru)

Hydrogenation of *p*-nitrophenol by gold nanoparticles immobilized within macroporous amphoteric cryogel based on N,N-dimethylaminoethylmethacrylate and methacrylic acid

Macroporous amphoteric cryogel based on N,N-dimethylaminoethylmethacrylate and methacrylic acid (DMAEM-MAA) was used for immobilization of gold nanoparticles (AuNPs). The structure of AuNPs immobilized within macroporous amphoteric cryogel represents the triangular, hexagonal, spherical and rod-like species the sizes of which are varied from 3 to 10 μm. Amphoteric cryogel with immobilized AuNPs was tested as flow-through catalytic reactor in reduction of 4-nitrophenol by $NaBH_4$.

Key words: macroporous amphoteric cryogels, gold nanoparticles, catalytic activity, flow-through reactor.

Introduction

Information on stabilization of AuNPs by amphoteric polyelectrolytes is very limited. A new regular polyampholyte, namely poly-(N,N-diallyl-N,N-dimethylammonium-alt-N-octyl-maleamic carboxylate) is proved to be an efficient reducing and stabilizing agent for the formation of gold colloids [1]. Water-soluble and durable Au nanoclusters, smaller than 4 nm with a narrow size distribution, were supported on a pH- and solvent-responsive water-soluble polyampholyte (SPES) [2]. The phase separation and sensitivity of the SPES-stabilizing Au nanoclusters permitted a facile separation of the clusters from the reaction mixture without any negative aggregation. Diblock polyampholytes poly(methacrylic acid)-block-poly(N,N-dimethylaminoethyl methacrylate), having different molecular weight and block ratio were used for stabilization of AuNPs [3]. Supporting of noble and transition metal ions in bulk of amphoteric nano-, micro-, macrogels followed by reduction to zero-valent state will open new perspectives for development of effective catalytic systems for decomposition, isomerization, hydrogenation, and oxidation of various organic substrates [4–6]. In this context design of monolithic support with microporous structure that can provide both nanoparticle loading and liquid flux is challenging task. A considerable effort of researchers is devoted to construct the catalytic system that is highly active, selective, stable, easy to handle, reusable and simple to separate the product from the reaction medium [7]. Literature survey reveals that the most studied superporous cryogels for immobilization of metal nanoparticles exhibit anionic or cationic character. Superporous cryogels of poly(acrylic acid) [8], poly(4-vinylpyridine) [9] and poly(2-acrylamido-2-methyl-1-propansulfonic acid) [10] and their templated metal nanoparticle composites were used in hydrogen generation from the hydrolysis of $NaBH_4$ and hydrogenation of 4-nitrophenol. The idea of application of amphoteric macroporous cryogels with immobilized nanoparticles of metals as flowing reactors in catalysis was outlined for the first time in our previous publications [4–6] and mentioned only in passing for chitosan-based cryogels [11].

In the present communication we report for the first time the catalytic activity of AuNPs immobilized within cryogel matrix in reduction of 4-nitrophenol.

Experimental section

Materials and Methods. Monomers, catalyst and initiator — methacrylic Acid (MAA, 99 % purity), N,N-dimethylaminoethylmethacrylate (DMAEM, 99 % purity), N,N,N',N'-tetramethylethylenediamine (TMED, 99 % purity), ammonium persulfate (APS, 99 % purity), and crosslinking agent N,N'-methylenbisacrylamide (MBAA, 99 % purity) — were purchased from Sigma-Aldrich Chemical Co., Milwaukee, WI, USA and used without further purification. Standard aqueous solution of tetrachlorauric acid $HAuCl_4$ with concentration 100 $mg \cdot L^{-1}$, *p*-nitrophenol (*p*-NPh) and sodium boronhydride ($NaBH_4$) were pur-

chased from Sigma-Aldrich. Concentration of gold in supernatant was determined by ion-coupled plasma atomic emission spectroscopy ICP-AES «Optima 5100DV» (Perkin Elmer, USA). Scanning electron microscopy (SEM) images were recorded on a JEOL JSM–6490LA (Japan) and on a high resolution SEM **(**Zeiss Merlin High-resolution SEM).

Synthesis of Amphoteric Cryogels. Mixture of MAA (343 mg or 4 mmol), DMAEM (626 mg or 4 mmol), MBAA (31 mg or 0.2 mmol) corresponding to molar ratio of monomers MAA:DMAEM = = 50:50 mol.%/mol.% was dissolved in 9 mL of deionized water, bubbled by nitrogen during 10 min and degassed under vacuum for about 5 min to eliminate the dissolved oxygen. After addition of 10 μL of TMED the solution was cooled in an ice bath for 5 min. Then 0.1 mL of aqueous solution of APS (10 wt.%) preliminary cooled in an ice bath for 5 min was added and the reaction mixture was stirred for 5 min. The total volume of reaction mixture was divided into 10 parts and each part containing 1 mL of reaction mixture was placed into the 10 glass cylinder with diameter 5 mm with closed outlet at the bottom. The solution in glass cylinder was frozen at minus 12 °C followed by cryopolymerization on cryothermostate Lauda Proline RP 845 (Germany) during 48 h. After completion of the reaction the sample was thawed at room temperature. The prepared cryogel sample was washed out thoroughly by distilled water every 2–3 hours during several days then successively washed out by 25, 50, 75 and 96 % ethanol to dehydrate then dried in air and finally in vacuum oven to constant mass at room temperature. Thus amphoteric cryogel with initial molar ratio of [MAA]:[DMAEM] = 50:50 mol.%/mol.% crosslinked by 5 mol.% of MBAA was synthesized (Fig. 1).

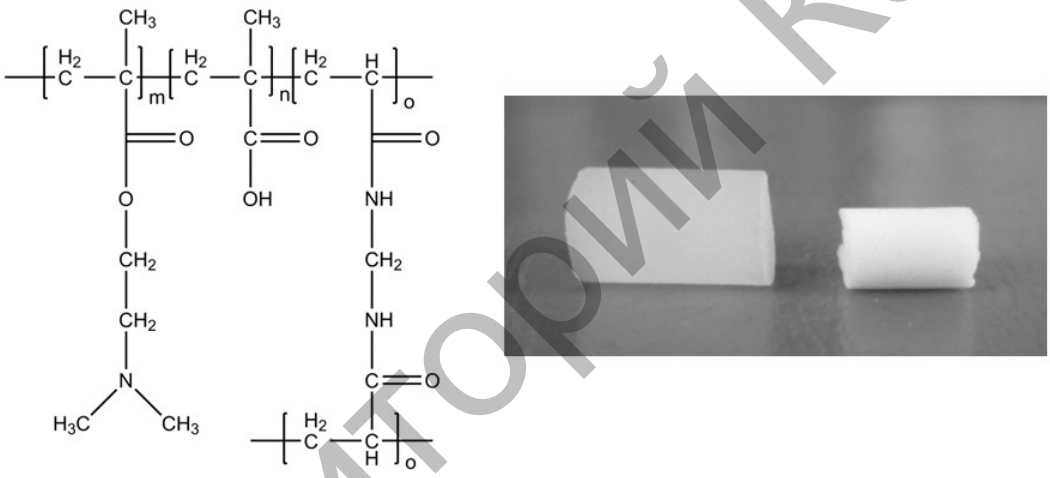

Figure 1. Structural units of amphoteric cryogels derived from MAA and DMAEM (left), dry and swollen in water cryogel samples (right)

Immobilization of AuNPs within the pores of DMAEM-MAA cryogel. 9.5 mL of deionized water was added to 0.5 mL $HAuCl_4$ with concentration 100 mg·L^{-1}. 0.5 g dry gel was immersed to 10 mL of prepared solution and boiled. After 30 min boiling the colorless DMAEM-MAA cryogel turned into raspberry-red color that is specific for AuNPs due to surface plasmon resonance effect. Further the DMAEM-MAA cryogel with immobilized AuNPs is abbreviated as DMAEM-MAA/AuNPs.

Evaluation of the catalytic activity of DMAEM-MAA/AuNPs. 10 mL aqueous solution composed of 0.5 mL $1 \cdot 10^{-3}$ mol·L^{-1} *p*-NPh, 0.5 mL $1 \cdot 10^{-2}$ mol·L^{-1} $NaBH_4$ and 9 mL of deionized water was pumped through the flow-type reactor containing AuNPs with the help of peristaltic pump (the flowing rate is 1.5 mL·min^{-1}). The concentration of *p*-NPh and *p*-APh was determined spectrophotometrically at 400 and 300 nm respectively.

Results and discussion

Morphology of DMAEM-MAA cryogel and AuNPs immobilized macroporous cryogel. According to SEM images the average pore size of DMAEM-MAA sample is varied from 40 to 80 μm (Fig. 2a). The structure of AuNPs immobilized within macroporous amphoteric cryogel represents the myriads of gold nanoparticles distributed in both surface and inner parts of macropores (Fig. 2b). Most of them are triangulars although the hexagonal, spherical and rod-like species are observed (Fig. 2c). The bigger sizes of AuNPs triangles immobilized within DMAEM-MAA cryogels are varied from 3 to 10 μm.

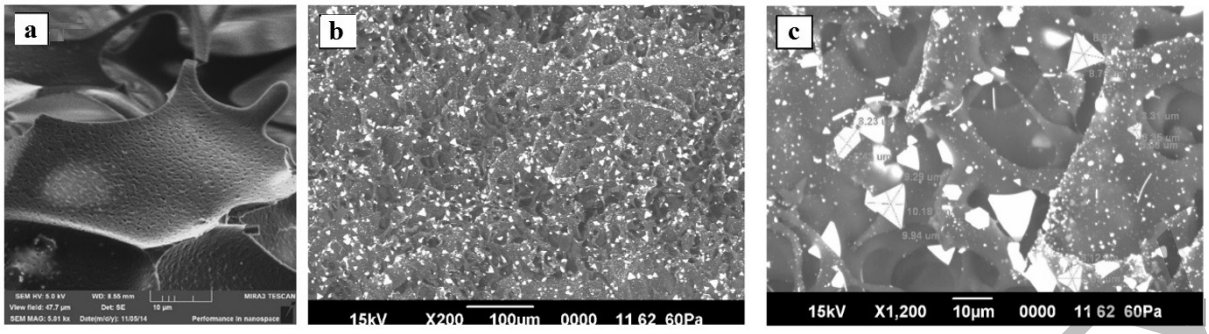

Figure 2. Morphology of pristine (*a*) and AuNPs immobilized macroporous amphoteric cryogel (*b*, *c*)

Catalytic activity of AuNPs immobilized within cryogel pores in hydrogenation of p-NPh. The reduction of *p*-NPh to *p*-APh by $NaBH_4$ (or hydrogen) as model reaction is easily monitored by measurement of the absorption spectra of substrate and reaction product at 400 and 300 nm respectively [12]. In our case the cryogel specimen containing AuNPs served as continuous-flow tank reactor for hydrogenation of *p*-NPh to *p*-APh. The flow-through catalytic reactor represents a glass tube with inner diameter 6–7 mm and height 100 mm which is filled by dry cryogel pieces with diameter 5 mm and height 10 mm. The bottom part of the glass tube is closed by Shott filter ended by valve. At first 10 or 15 mL of deionized water is passed through the cryogel sample. Due to quick swelling of cryogel the tight sealing between the inner wall of the glass tube and swollen sample takes place. Such simple construction allows the mixture of substrate and reducing agent to flow through the cryogel pores and to create enough contacts between the catalyst and reaction mixture. Passing of the mixture of *p*-NPh and $NaBH_4$ through amphoteric cryogel containing AuNPs immediately produces *p*-APh (Fig. 3a, b). The 95 % conversion is reached during 4 min after 5 times repeated passing of 10 mL mixture of *p*-NPh and $NaBH_4$ through the catalytic reactor (Fig. 3a). The same conversion degree is reached during 13 min after the successive fluxing of 50 mL mixture of *p*-NPh and $NaBH_4$ (Fig. 3b). The DMAEM-MAA/AuNPs preserved the high catalytic activity even after passing of 100 mL of *p*-NPh and $NaBH_4$ mixture. In our mind 100 % conversion of *p*-NPh is not reachable due to capturing of some amounts of substrate in deadly volume of cryogel. It should be noted that neither the mixture of *p*-NPh and $NaBH_4$ itself, nor the mixture of *p*-NPh and $NaBH_4$ fluxed through the DMAEM-MAA cryogel does not produce *p*-APh in absence of immobilized AuNPs.

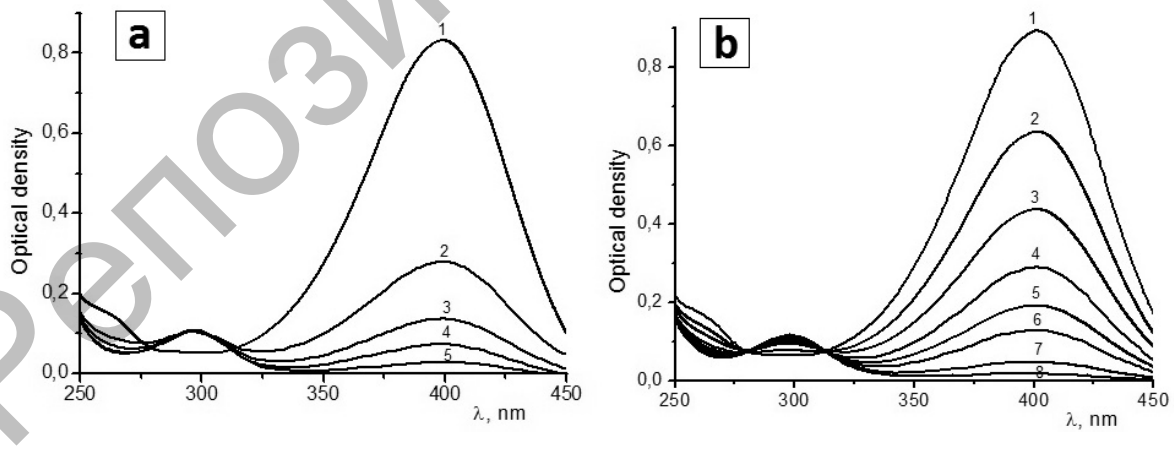

t, min: 0 (curve 1); 1 min (curve 2), 2 (curve 3), 3 (curve 4), 4 (curve 5), 5 (curve 6), 8 (curve 7), 11 (curve 8)

Figure 3. The time dependent absorbance spectra of *p*-NPh and *p*-APh during the 1st (*a*) and 5th (*b*) process cyclicity

The reduction rate constant of *p*-NPh has the pseudo-first-order and depends on the concentartion of nitrophenolate-anion rather than concentration of $NaBH_4$ due to its excess [12]. The kinetics of *p*-NPh reduction is expressed by equation:

$$\ln\left(\frac{C_t}{C_0}\right) = \ln\left(\frac{D_t}{D_0}\right) = -k \times t\,, \qquad (1)$$

where C_t and C_0 are concentrations of nitrophenolate-anions at definite time t and $t = 0$.

The logarithmic dependence of the equation (1) has linear character and shows that the first cycle is completed during 4 min with 95 % conversion, the second cycle — after 6 min, while the 95 % conversion of *p*-NPh to *p*-APh during 10 cycles requires 11 min (Fig. 4). The apparent rate constants (k_{app}) found from the slopes of kinetic curves of Figure 5 during the 1st, 2nd, 5th, and 10th reduction cycles of *p*-NPh are equal to $13.5 \cdot 10^{-3}$ s^{-1}; $8 \cdot 10^{-3}$ s^{-1}; $6.3 \cdot 10^{-3}$ s^{-1} $4.6 \cdot 10^{-3}$ s^{-1}. Thus, the k_{app} value decreases with increasing of process cyclicity. Cryogel catalyst sustained over 10 cycles without loss of activity.

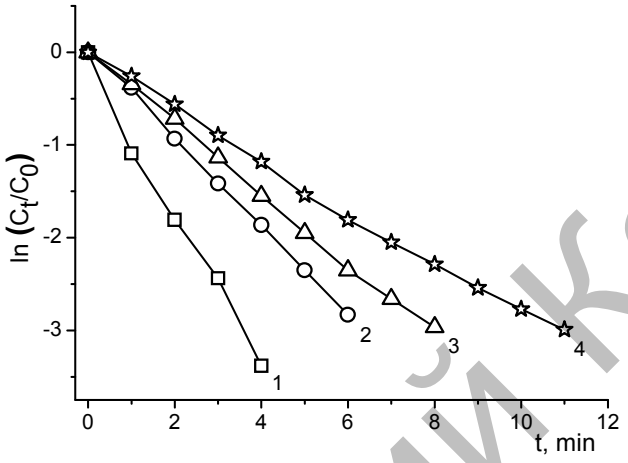

The 1st cycle (1), the 2nd cycle (2), the 5th cycle (3), the 10th cycle (4)

Figure 4. The reaction kinetic curves of $\ln(C_t/C_0)$ *versus* time as a function of process cyclicity

The kinetic rate constant of DMAEM-MAA/AuNPs for the reduction of *p*-NPh to *p*-APh was compared with literature data (see Table).

T a b l e

The rate constants of the reduction of *p*-NPh to *p*-APh catalyzed by metal nanoparticles supported on various polymers

Type of catalyst	Rate constant, $\times 10^{-2}$ s^{-1}	Ref.
PEI/AuNPs	4.6	[13]
PEI-C_{12}/AuNPs	5.2	[13]
HPEI-IBAM/AuNPs	≈ 2–3	[12]
Chitosan/AuNPs	0.24	[14]
Resin/AuNPs	2.5	[15]
Chitosan/FeNPs	0.24	[16]
PEC/AuNPs	0.5	[17]
PEC/PdNPs	0.394	
PEC/AgNPs	0.142	
PEC/$AuNPs_{50}$/$AgNPs_{50}$	0.678	
PEC/$AuNPs_{50}$/$AgNPs_{25}$/$PdNPs_{25}$	0.983	
PAMAM dendrimers/AuNPs	2.51	[18]
PAMAM dendrimers/AgNPs	0.71	
PAMAM dendrimers/CuNPs	2.43	
PD1–2/AuNPs	≈ 2.8	[19]
DMAEM-MAA/AuNPs	1.35	present work

Comparative analysis shows that DMAEM-MAA/AuNPs catalyst occupies intermediate position among the catalytic systems used for reduction of *p*-NPh to *p*-APh. It is commonly accepted that the reduc-

tion process involves chemisorption of 4-nitropenolate anions onto catalytic surface of AuNPs, interfacial electron transfer to reduce the 4-nitropenolate anions and desorption of 4-aminophenol from the surface. In our mind the *p*-NPh molecules are stabilized within the inner surface of DMAEM-MAA/AuNPs via hydrogen bonds between OH groups of substrate and COOH (or —$N(CH_3)_2$) groups of cryogel. The immobilized AuNPs in cryogel pores generates hydrogen atoms from the $NaBH_4$ that in its turn hydrogenate the nitro groups. Detachment of *p*-APh molecules from the surface of DMAEM-MAA/AuNPs takes place due to electrostatic repulsion, e.g. the negatively charged surface of AuNPs repels the same charged 4-nitrophenolate anions from the reaction mixture. The detailed mechanism of the reduction of *p*-NPh on the surface of AuNPs is given by authors. The lifetime of the catalyst is usually expressed through the turnover number (TON) that is the number of moles of substrate that a mole of the catalyst can convert before inactivation [20].

The stability of DMAEM-MAA/AuNPs catalyst, the so-called TON that is defined as

$$\mathrm{TON} = \frac{[p-\mathrm{NPh}]}{[\mathrm{AuNPs}]} \times \mathrm{OCT} \qquad (2)$$

(where [*p*-NPh] and [AuNPs] are the molar concentrations of substrate and catalyst, OCT is the overall catalytic time) and the turnover frequency (TOF) calculated (for the first cycle) according to equation

$$\mathrm{TOF} = \frac{[p-NPh]\cdot[conversion]}{[AuNPs]\cdot t} \qquad (3)$$

was equal to TON = 38,17 and TOF = 21,56 h^{-1} respectively.

Conclusions

Amphoteric cryogels of DMAEM-MAA were synthesized by cryopolymerization technique. SEM images of cryogels show sponge-like porous structure composed of interconnected channels. The structure AuNPs immobilized within the porous structure of cryogel is represented by triangular, hexagonal, spherical and rod-like species which play the role of catalytic centres in hydrogenation of substrates. The potential application of amphoteric cryogel samples with immobilized AuNPs as effective flow-through units for continuous hydrogenation of *p*-NPh is demonstrated.

Financial support from the Ministry of Education and Science of the Republic of Kazakhstan (1004/GF4 2015–2017) is greatly acknowledged.

References

1 *Note C., Koetz J., Wattebled L., Laschewsky A.* Effect of a new hydrophobically modified polyampholyte on the formation of inverse microemulsions and the preparation of gold nanoparticles // J. Colloid and Interface Sci. — 2007. — Vol. 308. — P. 162–169.

2 *Li S., Wu Y., Wang J., Zhang Q., Kou Y., Zhang S.* Double-responsive polyampholyte as a nanoparticle stabilizer: Application to reversible dispersion of gold nanoparticles // J. Mater. Chem. — 2010. — Vol. 20. — P. 4379–4384.

3 *Mahltig B., Cheval N., Gohy J.F., Fahmi A.* Preparation of gold nanoparticles under presence of the diblock polyampholyte PMAA-b-PDMAEMA // J. Polym. Res. — 2010. — Vol. 17. — P. 579–588.

4 *Kudaibergenov S.E., Nuraje N., Khutoryanskiy V.V.* Amphoteric nano-, micro- and macrogels, membranes, and thin films // Soft Matter. — 2012. — Vol. 8. — P. 9302–9321.

5 *Tatykhanova G., Sadakbayeva Zh., Berillo D., Galaev I., Abdullin Kh., Adilov Zh., Kudaibergenov S.* Metal Complexes of Amphoteric Cryogels based on Allylamine and Methacrylic Acid // Macromolecular Symposia. — 2012. — Vol. 317–318. — P. 7–17.

6 *Kudaibergenov S., Adilov Zh., Berillo D., Tatykhanova G., Sadakbaeva Zh., Abdullin Kh., Galaev I.* Novel Macroporous Amphoteric Gels: Preparation and Characterization // eXPRESS Polymer Letters. — 2012. — Vol. 6, No 5. — P. 346–353.

7 *Koga H., Kitaoka T.* One-step synthesis of gold nanocatalysts on a microstructured paper matrix for the reduction of 4-nitrophenol // Chem. Eng. J. — 2011. — Vol. 68. — P. 420–425.

8 *Sahiner N., Seven F.* The Use Of Superporous P(Aac(Acrylic Acid)) Cryogels As Support For Co and Ni Nanoparticle Preparation And As Reactor In H-2 Production From Sodium Borohydride Hydrolysis // Energy. — 2014. — Vol. 71. — P. 170–179.

9 *Sahiner N., Yildiz S.* Preparation of Superporous Poly(4-Vinyl Pyridine) Cryogel And Their Templated Metal Nanoparticle Composites for H-2 Production Via Hydrolysis Reactions // Fuel Process. Technol. — 2014. — Vol. 126. — P. 324–331.

10 *Sahiner N., Seven F.* Energy And Environmental Usage of Super Porous Poly(2-Acrylamido-2-Methyl-1-Propan Sulfonic Acid) Cryogel Support // RSC Advances. — 2014. — Vol. 4. — P. 23886–23897.

11 *Berillo D., Mattiasson B., Kirsebom H.* Cryogelation of Chitosan Using Noble-Metal Ions: In Situ Formation of Nanoparticles // Biomacromolecules. — 2014. — Vol. 15. — P. 2246–2255.

12 *Liu X.-Y., Cheng F., Liu Y., Liu H.J., Chen Y.* Preparation and characterization of novel ther-moresponsive gold nanoparticles and their responsive catalysis properties // J. Mater. Chem. — 2010. — Vol. 20. — P. 360–368.

13 *Veerakumar P., Velayudham M., Lu K.-L., Rajagopal S.* Polyelectrolyte encapsulated gold nanoparticles as efficient active catalyst for reduction of nitro compounds by kinetic method // Appl. Catal., A. — 2012. — Vol. 439. — P. 197–205.

14 *Seoudi R., Said D.A.* Studies on the Effect of the Capping Materials on the Spherical Gold Nanoparticles Catalytic Activity // World J. Nanoscience Eng. — 2011. — Vol. 1. — P. 51–61.

15 *Shah D., Kaur H.* Resin-Trapped Gold Nanoparticles: An Efficient Catalyst for Reduction of Nitro Compounds and Suzuki-Miyaura Coupling // J. Mol. Catal. A: Chem. — 2014. — Vol. 381. — P. 70–76.

16 *Lu H., Xueliang Q.X., Wang W., Tan F., Xiao Z., Chen J.* Chitosan stabilised nanozero-valent iron for the catalytic reduction of p-nitrophenol // Micro & Nano Letters. — 2014. — Vol. 9, Iss. 7. — P. 446–450.

17 *Islam M.Sh., Choi W.S., Lee H.-J.* Nonstoichiometric polyelectrolyte complexes: Smart nanomaterials for alloy and multimetallic catalyst // International Journal of Materials, Mechanics and Manufacturing. — 2014. — Vol. 2, Iss. 1. — P. 1–4.

18 *Nemanashi M., Meijboom R.* Synthesis and characterization of Cu, Ag and Au dendrimer-encapsulatednanoparticles and their application in the reduction of 4-nitrophenolto 4-aminophenol // J. Colloid Interface Sci. — 2013. — Vol. 389. — P. 260–267.

19 *Liu Y., Fan Y., Yuan Y., Chen Y., Cheng F., Shi-Chun J.* Amphiphilic hyperbranched copolymers bearing a hyperbranched core and a dendritic shell as novel stabilizers rendering gold nanoparticles with an unprecedentedly long lifetime in the catalytic reduction of 4-nitrophenol // J. Mater. Chem. — 2012. — Vol. 22. — P. 21173–21182.

20 *Hagen J.* Industrial Catalysis — A Practical Approach, 2nd ed. — Wiley-VCH: Weinheim, 2006.

А.Н.Кливенко, Г.С.Татыханова, Нұршат Нұраджи, С.Е.Құдайбергенов

Алтынның нанобөлшектері иммобилденген N,N-диметиламиноэтилметакрилат және метакрил қышқылы негізіндегі макроторлы амфотерлі криогель көлемінде *n*-нитрофенолды гидрлеу

N,N-диметиламиноэтилметакрилат және метакрил қышқылы (МАҚ–ДМАЕМ) негізіндегі макроторлы амфотерлі криогель алтынның нанобөлшектерін иммобилизациялауға қолданылды. Макроторлы амфотерлі криогель көлеміндегі алтынның нанобөлшектері үшбұрышты, алтыбұрышты, сфералық және түтікше тәрізді күйде кездеседі және көлемдері 3 пен 10 мкм аралығында. Алтын нанобөлшектері иммобилизацияланған амфотерлі криогель үлгісін ағымды каталитикалық реактор ретінде 4-нитрофенолды $NaBH_4$ гидрлеу реакциясына сыналды.

А.Н.Кливенко, Г.С.Татыханова, Нуршат Нураджи, С.Е.Кудайбергенов

Гидрирование *n*-нитрофенола наночастицами золота, иммобилизованными в макропоры амфотерного криогеля на основе N,N-диметиламиноэтилметакрилата и метакриловой кислоты

Макропористый амфотерный криогель на основе N,N-диметиламиноэтилметакрилата и метакриловой кислоты (МАА–ДМАЕМ) использован для иммобилизации наночастиц золота. Структура иммобилизованных в макропоры амфотерного криогеля наночастиц золота представляет собой треугольные, шестиугольные, сферические и стержнеподобные частицы, размеры которых варьируются от 3 до 10 мкм. Амфотерный криогель с иммобилизованными наночастицами золота тестирован в качестве проточного каталитического реактора в реакции гидрирования 4-нитрофенола $NaBH_4$.